THE STROMLO–APM REDSHIFT SURVEY. I. THE LUMINOSITY FUNCTION AND SPACE DENSITY OF GALAXIES

J. LOVEDAY AND B. A. PETERSON

Mount Stromlo and Siding Spring Observatories, Private Bag, Weston Creek Post Office, ACT 2611, Australia

AND

G. EFSTATHIOU AND S. J. MADDOX

Department of Physics, Keble Road, Oxford, OX1 3RH, England, UK

Received 1991 August 14; accepted 1991 November 8

ABSTRACT

We present the first results from a new redshift survey of southern galaxies. The survey is essentially complete to a magnitude limit of $b_J = 17.15$ and consists of 1769 galaxies sampled randomly at a rate of 1 in 20 from the APM galaxy catalogs. Our survey samples a volume ~ 30 times larger than the 14.5 mag CfA Redshift Survey and so can provide an accurate determination of the luminosity function and mean space density of galaxies. After correction for Malmquist bias, the luminosity function is well fitted over the magnitude range $-15 > M_{b_J} > -22$ by a Schechter function with parameters $M_{b_J}^* = -19.50 \pm 0.13$, $\alpha = -0.97 \pm 0.15$, and $\phi^* = (1.40 \pm 0.17) \times 10^{-2}$ Mpc^{-3} for $H_0 = 100$ kms^{-1} Mpc^{-1}. We estimate the variation of galaxy density with redshift using a maximum-likelihood method. The absence of a large local void in our survey supports our previous conclusion that the galaxy population must evolve rapidly at relatively low redshifts ($z \sim 0.1$) to explain the observed number counts over the range $16 \lesssim b_J \lesssim 19$.

Subject headings: galaxies: distances and redshifts — galaxies: fundamental parameters — redshifts — surveys

1. INTRODUCTION

Several complete redshift surveys of galaxies have been constructed in the last decade. The Revised Shapley Ames Catalog (Sandage & Tammann 1987) and the larger 14.5 mag CfA and Southern Sky redshift surveys (Huchra et al. 1983; da Costa et al. 1988) sample nearby galaxies over a wide area of sky. Several "pencil-beam" surveys (e.g., Kirshner et al. 1979, 1983; Peterson et al. 1986; Metcalfe et al. 1989) have provided small but deep galaxy samples in selected regions of the sky. The new CfA2 Redshift Survey (Geller & Huchra 1989) aims to extend the original CfA Survey to a Zwicky magnitude limit of 15.5 thus increasing the volume sampled by a factor of ~ 5. In addition, two redshift surveys of *IRAS* galaxies have been completed recently (Strauss et al. 1990; Lawrence et al. 1991).

In this paper we describe the first results from a new redshift survey of optically selected galaxies. The survey differs from previous optical redshift surveys in that we have selected galaxies randomly at a rate of 1 in 20 from a complete magnitude-limited catalog. Our survey is thus analogous to the QDOT sparse-sampled redshift survey of *IRAS* galaxies (Lawrence et al. 1991). The advantages of sparse-sampling for studies of large-scale structure in the Universe have been discussed by Kaiser (1986). By sampling the galaxy distribution sparsely it is possible to survey a large volume of space, gaining information on large-scale structure at the expense of fine detail in the galaxy distribution. A sparse-sampled survey is also powerful for determining the luminosity function and mean space density of galaxies, since fluctuations arising from individual clusters and groups are much reduced compared with a fully sampled survey containing the same number of galaxies (Efstathiou et al. 1990).

Our redshift survey is described briefly in § 2. Estimates of the luminosity function and mean space density of galaxies are presented in § 3. In § 4 we derive the radial variation of the galaxy density in our survey and show how little this affects galaxy number counts at bright magnitudes.

2. THE STROMLO–APM REDSHIFT SURVEY

Our redshift survey is based on a catalog of bright galaxies (the APM Bright Galaxy Catalogue, Loveday 1989) selected from the APM Galaxy Survey (Maddox et al. 1990a) which was compiled from 185 UK SERC J-survey Schmidt plates.

The plates were scanned with the Automated Photographic Measurement (APM) system at Cambridge and cover 4300 square degrees of the southern sky approximately defined in equatorial coordinates by $21^h \lesssim \alpha \lesssim 5^h$, $-72°.5 \lesssim \delta \lesssim -17°.5$. To construct the APM Bright Galaxy Catalogue, every extended image with $b_J \lesssim 16.5$ was inspected by JL on film copies of the Schmidt plates and each galaxy assigned a morphological classification: early-type (elliptical-lenticular), late-type (spiral-irregular), merged, or uncertain. The criterion for selecting extended images (as opposed to stellar images) was chosen conservatively to reject less than $\sim 5\%$ of compact, high surface brightness galaxies. The visual inspection enables all nongalaxy images ($\sim 70\%$ of the candidates) to be rejected, thus ensuring that contamination by stars is negligible. This procedure is necessary for images brighter than $b_J \approx 16.5$ since halos around bright stellar images on Schmidt plates cause difficulties with star-galaxy classification using the measuring machine parameters alone. Photographic magnitudes have been converted to the total b_J system (Couch & Newell 1980) by comparison with CCD photometry obtained with the Mount Stromlo and Siding Spring Observatories (MSSSO) 40″ telescope between 1988 and 1990. Figure 1 shows a plot of the CCD magnitude against the APM magnitude for 252 galaxies and the line through the points shows the quadratic relation that we have used to convert the APM magnitudes to the Couch and Newell system. The scatter about this line in the
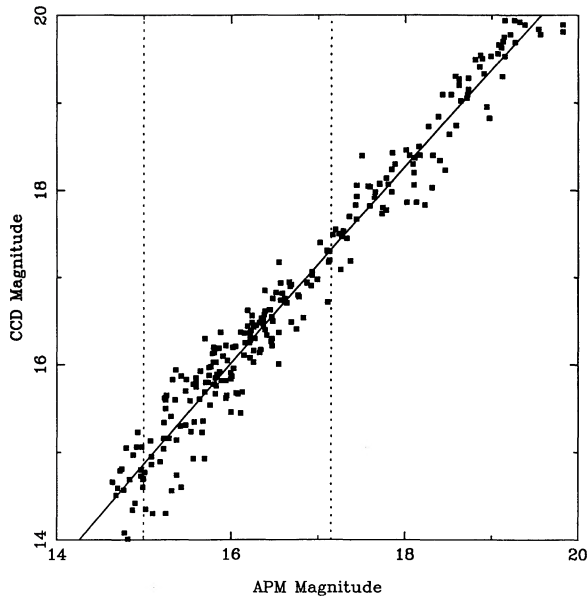
Fig. 1.—CCD magnitudes in the b_J system of Couch & Newell (1980) plotted against APM photographic magnitudes for 252 galaxies. The line shows the quadratic fit that we have used to convert the photographic magnitudes to the b_J system. The scatter about this line in the magnitude range $15 \leq b_J \leq 17.15$ (shown by the vertical dotted lines) is 0.30 mag.

magnitude range $15 \leq b_J \leq 17.15$ is 0.30 mag and this scatter is taken into account when fitting the luminosity function, as discussed below. Full details of star-galaxy separation, photometric matching, and calibration for the APM Bright Galaxy Catalogue are described by Loveday (1989) and will be published elsewhere.

To form the redshift survey sample, galaxies were selected at random from the APM Bright Galaxy Catalogue at a rate of 1 in 20. To extend the redshift survey to fainter magnitudes, we selected objects at the same sampling rate from the deeper APM Galaxy Survey that were brighter than $b_J = 17.15$ but not included in the Bright Galaxy Catalog. After visual inspection of these objects (by SJM) we ended up with a homogeneous random sample of 2002 galaxies. Of these galaxy images, 205 were observed to be merged with other objects on the Schmidt plates, 70.5% of which are stars. Because it is difficult to measure magnitudes and redshifts for overlapping images, we are currently omitting these objects from our analysis, leaving a sample of 1797 unmerged galaxies. To date, 1758 galaxies have been observed with the MSSSO 2.3 m telescope and double beam spectrograph over 39 nights from 1987 November to 1991 September. Redshifts were determined using cross-correlation techniques (Tonry & Davis 1979) and by measurement of emission lines. Reliable redshifts (rms velocity error ~ 50 km s^{-1}) have been obtained for 1719 spectra. In addition, 50 galaxies in our sample had redshifts already measured for the Southern Sky Redshift Survey (SSRS; da Costa et al. 1988). Our redshift survey is currently 98.5% complete (1769 out of 1797 galaxies) and the median redshift is 15,200 km s^{-1}. The small degree of incompleteness at the faint end is allowed for in our analysis by setting the magnitude limit m_0 for incomplete Schmidt fields to be the average of the magnitudes of the faintest galaxy in that field with a redshift and the next faintest galaxy.

In Figure 2 we show cone plots of the galaxy distribution in four declination slices where the declination limits have been

chosen to give roughly equal numbers of galaxies in each plot. Note that the survey edges are defined by the boundaries of individual Schmidt plates rather than by lines of constant right ascension, hence the galaxy density appears low at the edges of the plots. Despite our sparse-sampling strategy, large-scale structures are clearly visible in these plots. A quantitative analysis of large-scale galaxy clustering in the Stromlo–APM Redshift Survey will be the subject of a future paper (Loveday et al. 1992).

3. THE GALAXY LUMINOSITY FUNCTION

We have estimated the galaxy luminosity function $\phi(L)$ from the Stromlo–APM Redshift Survey using the Sandage, Tammann, & Yahil (1979) STY parametric maximum-likelihood method and the step-wise maximum likelihood (SWML) method of Efstathiou, Ellis, & Peterson (1988; hereafter EEP). These estimators are unbiased by density inhomogeneities and have well-defined error properties. In both methods we assume that $\phi(L)$ has a universal form, i.e., the number density of galaxies is separable into a function of luminosity times a function of position: $n(L, x) = \phi(L)\rho(x)$. Using these estimators, the shape of $\phi(L)$ is determined independently of its normalization.

3.1. Shape

The probability of seeing a galaxy of luminosity L_i at redshift z_i in a flux-limited catalog is given by

$$p_i \propto \phi(L_i) \Big/ \int_{L_{min}(z_i)}^{L_{max}(z_i)} \phi(L)dL \,, \qquad (1)$$

where $L_{min}(z_i)$ and $L_{max}(z_i)$ are the minimum and maximum luminosities observable at redshift z_i in a flux-limited sample. In the STY method, the likelihood $\mathscr{L} = \prod p_i$ (where the product extends over all galaxies in the sample) is maximized with respect to a set of parameters describing the function $\phi(L)$. For example, if we assume that $\phi(L)$ is described by a Schechter (1976) function,

$$\phi_S(L)dL = \phi^* \left(\frac{L}{L^*}\right)^\alpha \exp\left(-\frac{L}{L^*}\right) d\left(\frac{L}{L^*}\right), \qquad (2)$$

we maximize the likelihood with respect to α and L^* (or M^* in magnitudes). The effect of random error in our magnitudes is to convolve the "true" luminosity function with the magnitude error distribution. We assume that our magnitude errors are distributed as a Gaussian with zero mean and rms $\sigma_m = 0.30$ (see Fig. 1). The observed luminosity function $\phi_0(M)$ is then given by

$$\phi_0(M) = \frac{1}{\sqrt{2\pi}\sigma_m} \int_{-\infty}^{\infty} \phi_S(M') \exp\left[\frac{-(M' - M)^2}{2\sigma_m^2}\right] dM' \,. \qquad (3)$$

By fitting this convolved function to our observations, the Schechter function $\phi_S(L)$ thus determined will describe the "true" luminosity function which would have been measured directly from the data in the absence of magnitude errors, and thus corrects for Malmquist bias.

To provide a check of the functional form of $\phi(L)$, we have used the SWML method of EEP in which $\phi(L)$ is parameterized as a set of numbers ϕ_k in equally spaced magnitude bins. The likelihood $\mathscr{L}$ is maximized with respect to ϕ_k applying constraints as described in EEP. EEP describe in detail how to obtain error estimates from the information matrix and

$-72.5 < \delta < -52.0$

$-40.0 < \delta < -28.0$

$-52.0 < \delta < -40.0$

$-28.0 < \delta < -17.5$

FIG. 2a

FIG. 2b
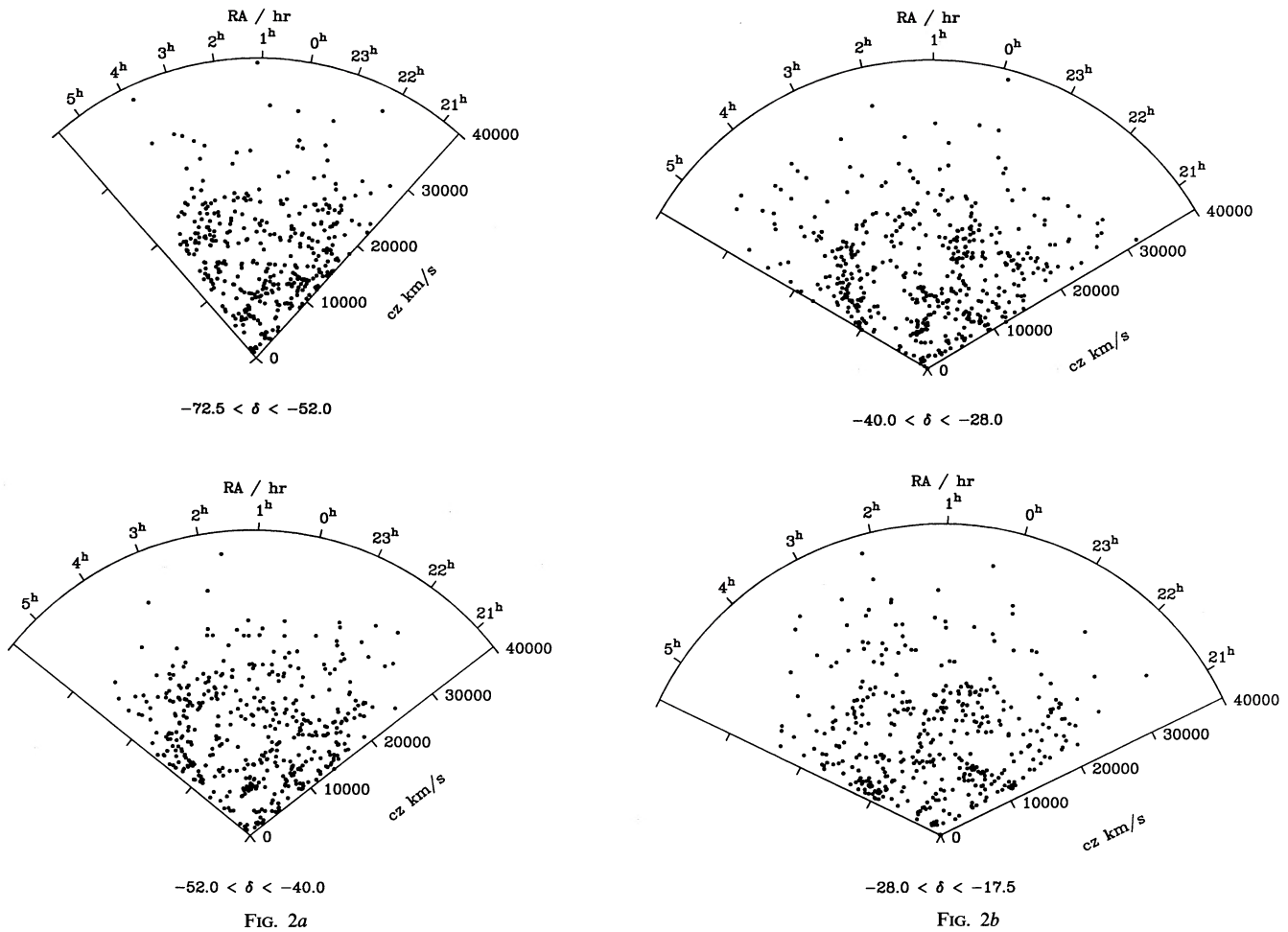
FIG. 2.—(a–b) Cone plots of the galaxy distribution in right ascension–redshift space for four slices in declination

a goodness of fit comparison with an assumed parametric form such as equations (2) or (3).

Our estimates of $\phi(L)$ are based on 1658 galaxies in the distance range $5 < x < 400 \; h^{-1}$ Mpc (where x is the comoving coordinate distance) with absolute magnitudes $-22 < M < -15$ and apparent magnitudes $15 < b_J < 17.15$. We apply a bright apparent magnitude limit to exclude galaxies which are saturated on the photographic plates (see Fig. 1). Measured radial velocities are transformed to the local group frame using $v = v + 300 \sin (l) \cos (b)$ and we assume $\Lambda = 0$, $q_0 = 0.5$ and $H_0 = 100$ km s^{-1} Mpc^{-1} with uniform Hubble flow in calculating distances. We adopt k-corrections for different morphological types in the b_J system as described in EEP.

In Figure 3 the symbols with error bars show $\phi(L)$ determined using the SWML estimator for all galaxies in the sample and for early-type (elliptical and lenticular) and late-type (spiral and irregular) galaxies. The solid lines show best-fitting pure Schechter functions (eq. [2]) and the dashed lines show best-fitting convolved Schechter functions (eq. [3]), both determined from the STY method. It can be seen that the convolved form of the Schechter function provides a rather better fit to the step-wise estimates of $\phi(L)$ than does a pure Schechter function, which falls too steeply at bright magnitudes. The main effect of the convolution is to "flatten out" the lumi-

nosity function, providing a better fit to the observations. The inset in Figure 3a shows the error contours for the corrected Schechter parameters. The parameters for these Schechter function fits, together with 1 σ likelihood errors are listed in Table 1. The "uncorrected" Schechter parameters are those determined by fitting equation (2) to the observations, and so are affected by Malmquist bias. The "corrected" parameters are those describing a Schechter function which, when convolved with a Gaussian with $\sigma_m = 0.30$, provides a maximum-likelihood fit to the observations. The bias in α and M^* caused by magnitude errors is fairly small, being roughly equal in amplitude to the 1 σ likelihood errors.

Table 1 also lists Schmidt's (1968) $\langle V/V_{max} \rangle$ statistic for each sample. Note that for early-type galaxies, $\langle V/V_{max} \rangle = 0.32$, showing that there is a bias against identifying these galaxies at large distances. This is not too surprising, given the difficulty in classifying $b_J \approx 17$ galaxies from Schmidt plates; many of these galaxies will have been assigned an "uncertain" morphological classification. Nevertheless, provided that the loss of early-type galaxies at each apparent magnitude is independent of intrinsic luminosity there should be no bias in our estimate of the luminosity functions since radial variations in the galaxy density cancel in equation (1). The results of Table 1 are in good agreement with those of EEP, though our new determinations have much smaller uncertainties. Note also that EEP
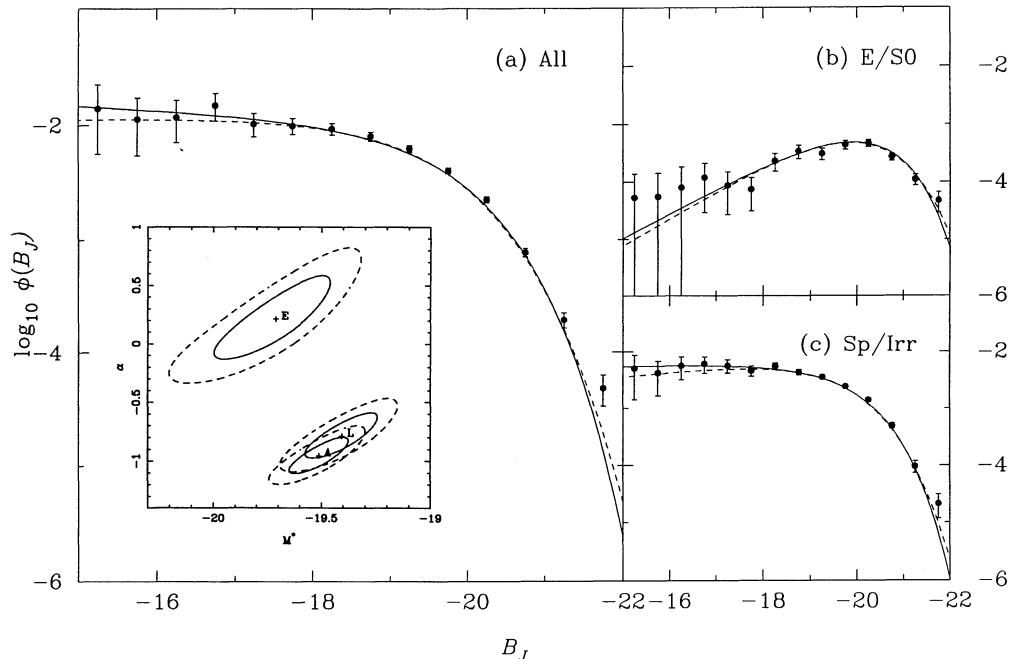
FIG. 3.—Step-wise maximum-likelihood estimates of the field galaxy luminosity function for (a) all galaxy types, (b) early types (E/S0), and (c) late types (Sp/Irr). The solid and dashed lines show the best-fitting pure and convolved Schechter functions, respectively, with parameters listed in Table 1. The inset in (a) shows the 1 σ (solid lines) and 2 σ (dotted lines) error contours for the corrected Schechter function parameters (see EEP eq. [2.7]).

found a shallow faint end slope ($\alpha \approx -0.48 \pm 0.5$) for the luminosity function of early-type galaxies, consistent with our results. Our results for early and late-type galaxies are also consistent with the luminosity functions presented for more finely divided morphological types by Binggeli, Sandage, & Tammann (1988).

3.2. Normalization

We determine the normalization ϕ^* of the Schechter function (eq. [2]) using the following estimator of the space density of galaxies:

$$f\bar{n} = \sum_{i=1}^{N_{gal}} w(x_i) \bigg/ \int_{x_{min}}^{x_{max}} dV S(x)w(x) , \qquad (4)$$

where f is the sampling rate, $S(x)$ the galaxy selection function and $w(x)$ a weighting function. The selection function for galaxies with luminosities L_1 to L_2 is

$$S(x) = \int_{\max (L_{min}(x), L_1)}^{\min (L_{max}(x), L_2)} \phi(L)dL \bigg/ \int_{L_1}^{L_2} \phi(L)dL . \qquad (5)$$

We adopt the weighting function

$$w(x) = \frac{1}{[1 + 4\pi f\bar{n}J_3(r_c)S(x)]} , \quad J_3(r_c) = \int_0^{r_c} r^2 \xi(r)dr , \quad (6)$$

where $\xi(r)$ is the two-point galaxy correlation function. Provided $J_3(r_c)$ converges on a scale r_c much smaller than the depth of the survey, then the weighting scheme (eq. [6]) minimizes the variance in the estimate of $\bar{n}$ (Davis & Huchra 1982). Of course, we cannot estimate J_3 on scales comparable to the survey volume and so one cannot *guarantee* that equation (6) will provide a minimum variance estimate. We use galaxies in the distance range $5 \le x \le 400 \; h^{-1}$ Mpc and adopt $4\pi J_3 \approx 10{,}000 \; h^{-3}$ Mpc³. The latter value comes from integrating the redshift-space two-point galaxy correlation function from our survey (Loveday et al. 1992) to $r_c \approx 20 \; h^{-1}$ Mpc; at larger separations the value of J_3 becomes uncertain. However, the results are insensitive to the value of J_3, changing by only 3% if J_3 is doubled.

The density $\bar{n}$ is determined by iteration from equations (4)–(6) to be $\bar{n} = 5.52 \times 10^{-2} \; h^3$ Mpc⁻³ for $S(x)$ determined from a

TABLE 1

SCHECHTER FUNCTION SHAPE PARAMETERS

SAMPLE	N_g[a]	$\langle V/V_{max}\rangle$	UNCORRECTED			CORRECTED		
			α	M^*	P[b]	α	M^*	P[b]
All	1658	0.50	-1.11 ± 0.15	-19.73 ± 0.13	0.25	-0.97 ± 0.15	-19.50 ± 0.13	0.65
Early	311	0.32	$+0.06 \pm 0.35$	-19.84 ± 0.25	0.60	$+0.20 \pm 0.35$	-19.71 ± 0.25	0.64
Late	999	0.47	-0.93 ± 0.20	-19.62 ± 0.16	0.76	-0.80 ± 0.20	-19.40 ± 0.16	0.87

[a] The number of galaxies used in each sample.

[b] The probability of $\phi(L)$ being accurately described by a Schechter function as determined from the likelihood ratio test (see EEP).

pure Schechter function and $\bar{n} = 4.70 \times 10^{-2}$ h^3 Mpc^{-3} for $S(x)$ determined from the corrected Schechter function. The variance in $\bar{n}$ is

$$\text{var}\,(\bar{n}) = \frac{\bar{n} \int w^2 S\, dV + f\bar{n}^2 \int S_1 S_2\, w_1 w_2\, \xi(r_{12}) dV_1\, dV_2}{f(\int wS\, dV)^2}$$

$$\approx \frac{\bar{n}}{f \int wS\, dV}\, , \quad (7)$$

where the approximate expression holds if J_3 has converged. We find that $\delta\bar{n}/\bar{n} \approx 0.05$ with our chosen value of J_3.

For a Schechter luminosity function,

$$\phi^* = \bar{n}/[\Gamma(\alpha + 1, L_1/L^*) - \Gamma(\alpha + 1, L_2/L^*)]\, , \quad (8)$$

where Γ is the incomplete gamma function. For the convolved Schechter function, the gamma function is replaced by a numerical integration over equation (3) with ϕ^* set equal to unity. The normalization ϕ^* given by equation (8) is $\phi^* = 1.12 \times 10^{-2}$ h^3 Mpc^{-3} for the uncorrected Schechter function and $\phi^* = 1.40 \times 10^{-2}$ h^3 Mpc^{-3} for the corrected Schechter function. The error in ϕ^* due to the uncertainties in α and M^* is 11% and so combining this with the 5% error in $\bar{n}$, the overall uncertainty in ϕ^* is $\sim 12\%$. We thus conclude that $\phi^* = (1.40 \pm 0.17) \times 10^{-2} h^3$ Mpc^{-3}.

In order to see if our estimates of $\bar{n}$ and ϕ^* are affected by Malmquist bias, we have performed a series of Monte Carlo simulations. We generate a uniform, random distribution of points inside the survey volume and assign each point an absolute magnitude drawn randomly from a Schechter function with $\alpha = -0.97$ and $M^* = -19.50$. Each point is then either accepted or rejected, depending on whether or not its apparent magnitude lies in the range 15–17.15. A second flux-limited catalogue is generated from the same parent distribution after applying a magnitude error to each point drawn from a Gaussian distribution with zero mean and 0.30 rms. Five such pairs of simulated catalogs were produced, each containing ~ 8000 points. The parameters α, M^*, $\bar{n}$, and ϕ^* were determined for each simulation in the same way as for the survey data, fitting a pure Schechter function to the error-free simulations and a convolved Schechter function to the perturbed simulations. The results from these simulations are shown in Table 2, where the errors now come from the dispersion of the parameters determined from the individual simulations. This experiment verifies that our procedure of fitting a convolved Schechter function to the observations does indeed correct the shape of the luminosity function for the assumed magnitude errors and, moreover, that the correct normalization ϕ^* and density $\bar{n}$ are also determined.

4. RADIAL DENSITY VARIATION

Just as the maximum-likelihood estimate of $\phi(L)$ is independent of inhomogeneities in the galaxy distribution, one can also estimate the radial density $\rho(x)$ independently of the
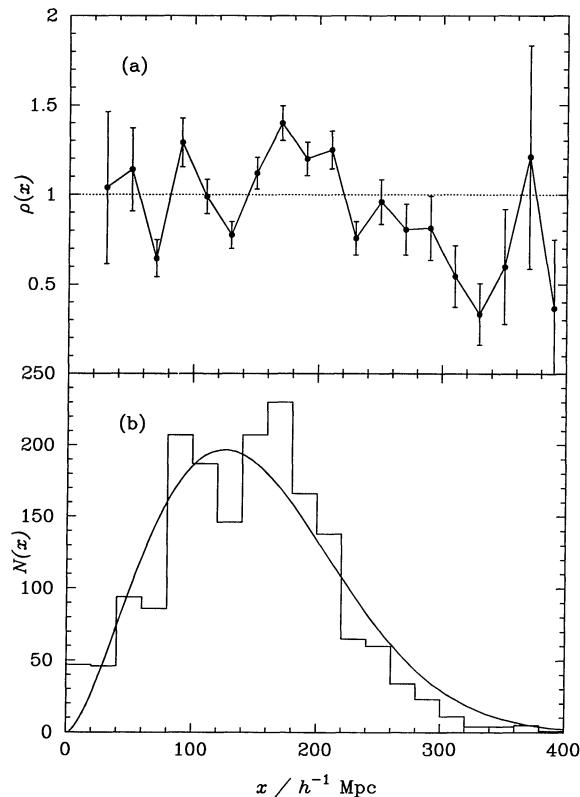
FIG. 4.—(a) The maximum-likelihood estimate of radial density in our redshift survey (eq. [9]). (b) The predicted and observed distance histogram for all galaxies in the redshift survey to 400 h^{-1} Mpc.

assumed luminosity function by maximizing the likelihood

$$\mathcal{L} = \prod_i \rho(x_i) \Big/ \int_{x_{\min}(L_i)}^{x_{\max}(L_i)} \rho(x) dV\, , \quad (9)$$

where $x_{\min}(L_i)$ and $x_{\max}(L_i)$ are the limiting distances at which a galaxy of luminosity L_i would still be included in the survey. We fitted $\rho(x)$ by an arbitrary step function, using a variant of the SWML estimator (Saunders et al. 1990). As in the maximum-likelihood estimate of $\phi(L)$, overall normalization is lost, and so we have applied the constraint

$$\int \rho(x)S(x)w(x)dV \Big/ \int S(x)w(x)dV = 1\, , \quad (10)$$

where $w(x)$ is the weighting function defined by equation (6). This constraint is also used for the error estimates (see EEP) which for our survey are close to the Poisson errors. Our estimate of $\rho(x)$ is plotted in Figure 4a and shows evidence for fluctuations at $\sim 30\%$ level on scales of ~ 50 h^{-1} Mpc. As an alternative way of presenting the radial density variation in the survey, in Figure 4b we plot the observed and predicted dis-

TABLE 2

RESULTS FROM MONTE CARLO SIMULATIONS

Sample	N_g	α	M^*	$\bar{n}$	$\phi^*/10^{-2}$
No mag error	7556 ± 61	-0.97 ± 0.04	-19.48 ± 0.03	0.26 ± 0.02	7.75 ± 0.28
0.3 mag error	8048 ± 118	-0.96 ± 0.05	-19.49 ± 0.04	0.25 ± 0.02	7.63 ± 0.49

NOTE.—Parameters for error-free simulations were determined from pure Schechter function fits, those for simulations with magnitude errors from convolved Schechter function fits.
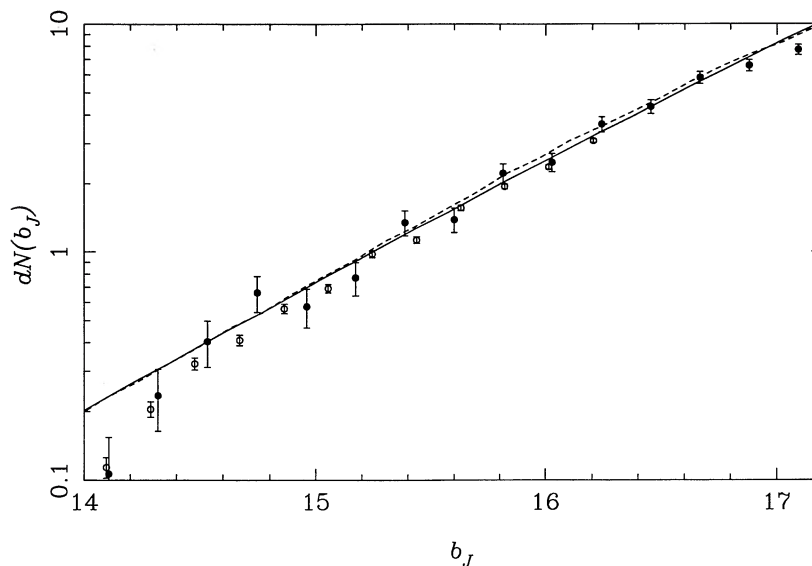
FIG. 5.—Comparison of observed and predicted number counts. The open symbols show counts from the APM Bright Galaxy Catalogue to its completeness limit and the solid symbols show counts from the Stromlo–APM Redshift Survey, divided by the sampling rate. The solid line shows predicted counts assuming our maximum-likelihood estimate of a convolved Schechter luminosity function, a homogeneous universe and a mean k-correction of $3z$; the dashed line includes the observed variation of the galaxy density with radial distance shown in Fig. 4a.

tance distributions. The predicted distribution is given by

$$N(x)dx = \omega x^2 \int_{L_{min}(x,\, m_0)}^{L_{max}(x,\, m_0)} \phi(L)dL \, , \qquad (11)$$

where $\omega \approx 1.31$ Sr is the survey solid angle. This plot shows all galaxies in the survey out to $400\, h^{-1}$ Mpc, whether or not they were included in the luminosity function determination. The fluctuations in observed radial density compared with a uniform universe are in excellent agreement with the luminosity function-independent estimator of radial density shown in Figure 4a. In Figure 5 we compare our observed and predicted number-magnitude counts. The solid symbols show counts from the redshift survey, multiplied by 20 to allow for sparse sampling and the open symbols show counts from the full APM Bright Galaxy Catalogue. The error bars are calculated assuming Poisson statistics. The predicted number counts are given by

$$n(m)dm = \int_0^{\infty} \phi[L(m, x)]\rho(x)dV \, . \qquad (12)$$

The solid line in Figure 5 shows equation (12) with $\rho(x) \equiv 1$ (i.e., a homogeneous universe) and the dashed line shows the counts predicted using the estimate of $\rho(x)$ shown in Figure 4a. The predicted counts agree extremely well with the observed counts over the magnitude range $14.5 < b_J < 17$. Brighter than $b_J = 14.5$ photographic saturation becomes a serious problem and fainter than $b_J = 17$ our survey is not quite complete. The radial density variations seen in our survey make only a small difference to the predicted number counts. We can therefore exclude convincingly the possibility of a "giant local void" as an explanation for the large excess in the number counts at 19th magnitude compared to no-evolution models normalized at 16th magnitude (Maddox et al. 1990b) implying that the shape of the luminosity function must have changed significantly by redshifts $z \sim 0.1$. Unfortunately, there are too few galaxies at redshifts $z \sim 0.1$ in the present survey to detect such luminosity evolution directly—the luminosity distribution test

described by Sandage, Tammann, & Yahil (1979) and Yahil et al. (1991) shows no evidence for variation of $\phi(L)$ with distance in our survey.

5. CONCLUSIONS

We have described the first results from the new Stromlo–APM Redshift Survey, which samples a significantly larger volume of space than any other optically selected redshift survey. We have shown that the b_J luminosity function is described accurately by a Schechter function over a wide range of absolute magnitudes $(-15 > M_{b_J} > -22)$. We find that $\phi(L)$ has a "flat" faint-end slope consistent with $\alpha = -1$ and we find evidence that the luminosity function of early-type galaxies differs from that of late-type galaxies. The large volume of the survey has enabled us to calculate the mean galaxy density to an accuracy of $\sim 5\%$, providing a very significant improvement over previous redshift surveys (see e.g. EEP).

A maximum-likelihood estimate of the radial density variations reveals relatively small inhomogeneities on the scale of the survey. These inhomogeneities make no significant difference to models of the galaxy number counts at bright magnitudes in the southern sky. These results and the low overall normalization of the local luminosity function found in our survey have important implications for the interpretation of number counts at fainter magnitudes. Our results strongly support the conclusion of Maddox et al. (1990b) that the rapid increase in number counts in the magnitude range $16 \lesssim b_J \lesssim 19$ can only be explained by significant evolution of the galaxy population at redshifts $z \sim 0.1$. A large change in the galaxy luminosity function at low redshifts would come as a surprise to many cosmologists, and it should be possible to check this directly with a redshift survey at $b_J \sim 19$.

LOVEDAY ET AL.

REFERENCES

Binggeli, B., Sandage, A., & Tammann, G. A. 1988, ARA&A, 26, 509
Couch, W. J., & Newell, E. B. 1980, PASP, 92, 746
da Costa, L. N., Pellegrini, P. S., Sargent, W. L. W., Tonry, J., Davis, M., Meiksin, A., & Latham, D. W. 1988, ApJ, 327, 544 (SSRS)
Davis, M., & Huchra, J. 1982, ApJ, 254, 437
Efstathiou, G., Ellis, R. S., & Peterson, B. A. 1988, MNRAS, 232, 431 (EEP)
Efstathiou, G., Kaiser, N., Saunders, W., Lawrence, A., Rowan-Robinson, M., Ellis, R. S., & Frenk, C. S. 1990, MNRAS, 247, 10P
Geller, M. J., & Huchra, J. P. 1989, Science, 246, 897
Huchra, J., Davis, M., Latham, D., & Tonry, J. 1983, ApJS, 52, 89
Kaiser, N. 1986, MNRAS, 219, 785
Kirshner, R. P., Oemler, A., & Schechter, P. L. 1979, AJ, 84, 951
Kirshner, R. P., Oemler, A., Schechter, P. L., & Schectman, S. A. 1983, AJ, 88, 1285
Lawrence, A., Rowan-Robinson, M., Crawford, J., Saunders, W., Ellis, R. S., Frenk, C. S., Parry, I., Efstathiou, G., & Kaiser, N. 1992, in preparation
Loveday, J. 1989, Ph.D. thesis, University of Cambridge
Loveday, J., Efstathiou, G., Peterson, B. A., & Maddox, S. J. 1992, in preparation

Maddox, S. J., Sutherland, W. J., Efstathiou, G., & Loveday, J. 1990a, MNRAS, 243, 692
Maddox, S. J., Sutherland, W. J., Efstathiou, G., Loveday, J., & Peterson, B. A. 1990b, MNRAS, 247, 1P
Metcalfe, N., Fong, R., Shanks, T., & Kilkenny, D. 1989, MNRAS, 236, 207
Peterson, B. A., Ellis, R. S., Efstathiou, G., Shanks, T., Bean, A. K., Fong, R., & Zen-Long, Z. 1986, MNRAS, 221, 233
Sandage, A., & Tammann, G. A. 1987, A Revised Shapley-Ames Catalog of Bright Galaxies (2d ed., Washington, DC: Carnegie Institution)
Sandage, A., Tammann, G. A., & Yahil, A. 1979, ApJ, 232, 352 (STY)
Saunders, W., Rowan-Robinson, M., Lawrence, A., Efstathiou, G., Kaiser, N., Ellis, R. S., & Frenk, C. S. 1990, MNRAS, 242, 318
Schechter, P. L. 1976, ApJ, 203, 297
Schmidt, M. 1968, ApJ, 151, 393
Strauss, M. A., Davis, M., Yahil, A., & Huchra, J. P. 1990, ApJ, 361, 49
Tonry, J., & Davis, M. 1979, AJ, 84, 1511
Yahil, A., Strauss, M. A., Davis, M., & Huchra, J. P. 1991, ApJ, 372, 380